

## **AN EXACT SYNTHESIS METHOD FOR DUAL-BAND CHEBYSHEV IMPEDANCE TRANSFORMERS**

**G. Castaldi**

Department of Engineering  
University of Sannio  
Corso Garibaldi 107, Benevento 82100, Italy

**V. Fiumara and I. Gallina**

Department of Environmental Engineering and Physics  
University of Basilicata  
viale dell'Ateneo Lucano 10, Potenza 85100, Italy

**Abstract**—We propose an exact synthesis method which allows the design of dual-band transformers with an arbitrary even number of uniform sections giving equi-ripple impedance matching in two separate bands centered at two arbitrary frequencies. This method is a generalization of the exact Collin-Riblet synthesis of Chebyshev single-band transformers. As compared to a single-band Collin-Riblet transformer encompassing both required passbands, the proposed design yields significantly better performance in terms of passband tolerance and width.

### **1. INTRODUCTION**

The multisection transformer is a standard tool in microwave engineering to obtain impedance matching in transmission line circuits supporting transverse electromagnetic (TEM) propagation [1, 2]. In the 1950s classical design methods, e.g., binomial and Chebyshev synthesis [1], were introduced to design transformers giving impedance matching in a single passband. Classical transformers consist of a cascade of uniform transmission line sections which are a quarter wave long at the central frequency of the matching band. Other methods to design multisection transformers consisting of uniform or nonuniform transmission line sections are dealt with in [3–5].

However, the above mentioned methods faced the problem of designing impedance transformers working in a single passband. On the other hand, in many cases of practical interest (cellular/PCS, WLAN, GSM/DCS and other dual-band applications [6–9]) impedance matching over two separate bands can be required. So, in the last years various design methods for dual-band impedance transformers have been proposed [10–14]. In particular, the synthesis problem of a dual-band two-section one-third wavelength transformer with the two bands centered at a given frequency  $f_1$  and at its first harmonic  $2f_1$  is dealt with in [10] and [11]. The more general problem of designing a transformer working in two bands centered at two arbitrary frequencies is solved in [12] and [13], but only for a two-section transformer. Finally, the problem of designing a transformer with an arbitrary even number of quarter-wavelength uniform sections working in two bands centered at two frequencies  $f_1$  and  $f_2 \leq 3f_1$  is solved in [14], but under the small-reflections approximation. In particular, the method introduced in [14] is a generalization of the standard approximate single-band Chebyshev transformer design [1] in which the input reflection coefficient obtained using the small-reflection approximation is expressed as a Chebyshev polynomial with argument  $\cos \theta$ ,  $\theta$  being the electrical length of the transformer sections. The basic idea of the dual-band synthesis in [14] consists in replacing the argument  $\cos \theta$  by a suitable second order polynomial in  $\cos \theta$ . Note that this method gives accurate results only if the range of the ratio  $Z_L/Z_0$  is about  $1/2 \leq Z_L/Z_0 \leq 2$ , where  $Z_L$  is the real valued impedance to be matched to the transmission line with real valued characteristic impedance  $Z_0$  [1].

In this paper we present a dual-band design method which overcomes the limits on the ratio of the impedances  $Z_L/Z_0$  and frequencies  $f_2/f_1$  of the procedure in [14]. The method is based on the exact Collin-Riblet design procedure [15, 16] which allows the characteristic impedances of the transformer sections to be iteratively calculated once the power loss ratio (the power available from the generator divided by the power delivered to the load) is given. In the exact synthesis of single-band equi-ripple transformers the power loss ratio is enforced to be a suitable function of the Chebyshev polynomial with argument  $\cos \theta$  [1]. Our method for the exact dual-band design is based (as in [14]) on replacing the argument  $\cos \theta$  by a suitable second order polynomial in  $\cos \theta$ . In this way, we can obtain impedance transformers, consisting of a cascade of  $N = 2M$  uniform transmission line sections which are a quarter wave long at the frequency  $f_0 = (f_1 + f_2)/2$ , working in two bands  $\Omega_1$  and  $\Omega_2$  centered at two arbitrary frequencies  $f_1$  and  $f_2$ , respectively, without

any restriction on the ratio  $Z_L/Z_0$  and on  $M$ .

In terms of passband tolerance (largest reflection coefficient absolute value) in the two required bands  $\Omega_1$  and  $\Omega_2$ , the  $N$ -section transformer obtained using our method outperforms the exact single-band Chebyshev  $N$ -section transformer whose passband encompasses both  $\Omega_1$  and  $\Omega_2$ , which is perhaps the most obvious alternative design. We also analyze the robustness of our method with respect to the absorption, showing that moderate dielectric losses in the transmission line sections do not significantly affect the transformer performance. Moreover, we explore the possibility of using our synthesis procedure also in the case of waveguiding structures supporting quasi-TEM propagation, showing that our method gives very good results in facing the impedance matching problem in microstrip line circuits.

The paper is organized as follows. Our method is introduced and discussed in Section 2. Results follow under Section 3. Section 4 deals with the design of microstrip transformers. Conclusions follow under Section 5.

## 2. AN EXACT DUAL-BAND CHEBYSHEV IMPEDANCE TRANSFORMER

In this section we present our method to design a dual-band Chebyshev impedance transformer based on the exact Collin-Riblet synthesis procedure [15, 16].

Consider the synthesis problem of an impedance transformer consisting of  $N$ -sections having the same electrical length  $\theta = 2\pi l/\lambda$ ,  $l$  and  $\lambda$  being the optical length of the sections and the wavelength in the vacuum, respectively, that matches a load of impedance  $Z_L$  to a transmission line of characteristic impedance  $Z_0$  (both  $Z_L$  and  $Z_0$  are assumed to be real-valued) in two separate equal-width frequency bands, namely  $\Omega_1 = [f_1 - \Delta f, f_1 + \Delta f]$  and  $\Omega_2 = [f_2 - \Delta f, f_2 + \Delta f]$ , where  $f_1$  and  $f_2$  are two arbitrary frequencies. Following the Collin-Riblet procedure, we consider the power loss ratio  $P_{LR}$  [1]

$$P_{LR}(\theta) = \frac{P_G}{P_L(\theta)} = \frac{1}{1 - |\Gamma(\theta)|^2} \quad (1)$$

where  $P_G$  and  $P_L$  are the power available from the generator and the power delivered to the load, respectively, and  $\Gamma$  is the input reflection coefficient. It can be shown that  $P_{LR}$  can be expressed as [16]

$$P_{LR}(\theta) = 1 + Q_N^2(\cos \theta) \quad (2)$$

where  $Q_N(\cdot)$  is an even or odd polynomial of order  $N$ . Once the polynomial  $Q_N(\cdot)$  is given, the Collin-Riblet design method

allows the characteristic impedances of the transformer sections to be calculated [15, 16].

The polynomial  $Q_N(\cdot)$  can be chosen so that the impedance matching condition is obtained in the two separate equal-width bands  $\Omega_1$  and  $\Omega_2$ . To this end, we choose  $N = 2M$  and  $l = c/(4f_0)$ , where  $c$  is the velocity of the light in the vacuum and  $f_0 = (f_1 + f_2)/2$ . The electrical length of each section is  $\theta = \pi f/(2f_0)$ , and the two bands  $\Omega_1$  and  $\Omega_2$  can be expressed in terms of the dimensionless variable  $\theta$ , namely  $\Theta_1 = [\theta_1 - \Delta\theta, \theta_1 + \Delta\theta]$  and  $\Theta_2 = [\theta_2 - \Delta\theta, \theta_2 + \Delta\theta]$ , where  $\theta_1 = \pi f_1/(2f_0)$ ,  $\theta_2 = \pi f_2/(2f_0) = \pi - \theta_1$  and  $\Delta\theta = \pi\Delta f/(2f_0)$ . In order to obtain an equi-ripple power loss ratio in the two bands  $\Theta_1$  and  $\Theta_2$ , we enforce

$$Q_{2M} = kT_M(a \cos^2 \theta + b) \quad (3)$$

where  $T_M$  is the  $M$ th-degree Chebyshev polynomial and  $a$ ,  $b$  and  $k$  are constants to be determined. Note that our method is a variation of the single-band Chebyshev synthesis, using the second order polynomial  $a \cos^2 \theta + b$  as the argument of the Chebyshev polynomial instead of the first order polynomial used for the single-band design [1]. In order to obtain the impedance matching in the two bands  $\Theta_1$  and  $\Theta_2$ , we enforce the condition  $-1 \leq a \cos^2 \theta + b \leq 1$  for  $\theta \in \Theta_1 \cup \Theta_2$ , which, in view of the symmetry of the polynomial  $a \cos^2 \theta + b$  with respect to  $\pi/2$ , can be obtained enforcing

$$\begin{cases} a \cos^2(\theta_1 - \Delta\theta) + b = -1 \\ a \cos^2(\theta_1 + \Delta\theta) + b = 1 \end{cases} \quad (4)$$

Equation (4) gives the constant  $a$  and  $b$

$$\begin{cases} a = \frac{2}{\cos^2(\theta_1 + \Delta\theta) - \cos^2(\theta_1 - \Delta\theta)} \\ b = -\frac{\cos^2(\theta_1 + \Delta\theta) + \cos^2(\theta_1 - \Delta\theta)}{\cos^2(\theta_1 + \Delta\theta) - \cos^2(\theta_1 - \Delta\theta)} \end{cases} \quad (5)$$

Finally, the constant  $k$  can be obtained by considering

$$P_{LR}(0) = \frac{|R+1|^2}{4R} \quad (6)$$

where  $R = Z_L/Z_0$ . Using Equations (2), (3) in (6) yields

$$k = \frac{|R-1|}{2\sqrt{R}|T_M(a+b)|} \quad (7)$$

Once the constants  $a$ ,  $b$  and  $k$  have been computed, the power loss ratio  $P_{LR}$  is completely determined and the characteristic impedances of the transformer sections can be computed using the Collin-Riblet method [15, 16].

### 3. REPRESENTATIVE RESULTS

As an illustration of our method, in this section we present some representative results. Given the two frequency bands  $\Omega_1$  and  $\Omega_2$  and the impedances  $Z_0$  and  $Z_L$ , following the method described in the above section we computed the characteristic impedances of the transformer sections. In all calculations we performed, the values of these impedances resulted to be real and positive according to the physical realizability stated by the Riblet theory. Once the characteristic impedances of the  $N$ -sections of the transformer had been computed, we calculated the input reflection coefficient of the transformer  $\Gamma_{in}(\theta)$  using the transmission matrix method [1]. In all simulations  $|\Gamma_{in}(\theta)|$  exactly agreed with the reflection coefficient absolute value  $|\Gamma(\theta)|$  obtained substituting Equations (3) and (2) in Equation (1), that is

$$|\Gamma(\theta)| = \frac{|kT_M(a \cos^2 \theta + b)|}{[1 + k^2 T_M^2(a \cos^2 \theta + b)]^{1/2}} \quad (8)$$

As a first case, we considered  $R = 4$ ,  $N = 4$ ,  $\theta_2/\theta_1 = 2.5$  and  $\Delta\theta/\theta_1 = 0.2$ . In Fig. 1,  $|\Gamma_{in}|$  of our dual-band exact Chebyshev transformer (henceforth called dual-band transformer) is displayed as a function of the electrical length  $\theta$  and compared to the one of a four section single-band exact Chebyshev transformer (henceforth called single-band transformer), synthesized using the exact Collin-Riblet method, with a passband  $\Theta$  encompassing both required passbands, i.e.,  $\Theta = [\theta_1 - \Delta\theta, \theta_2 + \Delta\theta]$ . The passband tolerance  $\rho_m$  of the dual-band transformer is about 6.3 dB lower than the single-band transformer one.

In order to perform an extensive comparison between the dual-band transformer and the single-band transformer, we analyzed the input reflection coefficient spectrum of both transformers by varying the parameters  $R$ ,  $N$ ,  $\Delta\theta/\theta_1$  and  $\theta_2/\theta_1$ . Fig. 2 shows the passband tolerance  $\rho_m$  of the dual-band transformer and the single-band transformer as a function of  $R$  for  $N = 4$ ,  $\theta_2/\theta_1 = 2.5$  and  $\Delta\theta/\theta_1 = 0.2$ . As expected, the  $\rho_m$  of both transformers increases with  $R$ , and the dual-band transformer outperforms the single-band transformer by roughly 6.3 dB for all  $R$  values.

Increasing the number of the sections  $N$ , obviously the  $\rho_m$  of both transformers decreases, while the difference between the  $\rho_m$  of the

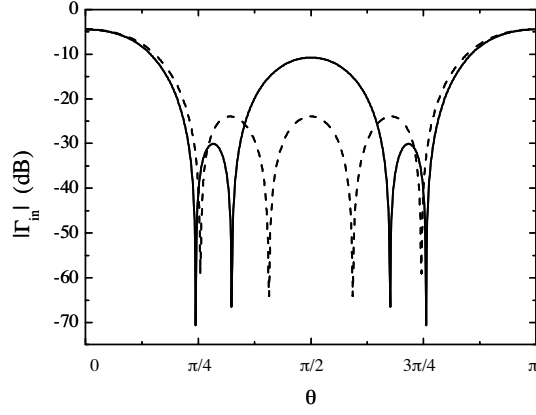


**Figure 1.** Reflection coefficient absolute value vs.  $\theta$  for the dual-band transformer (solid line) and the single-band transformer with passband  $[\theta_1 - \Delta\theta, \theta_2 + \Delta\theta]$  (dashed line) for  $R = 4$ ,  $N = 4$ ,  $\theta_2/\theta_1 = 2.5$  and  $\Delta\theta/\theta_1 = 0.2$ .

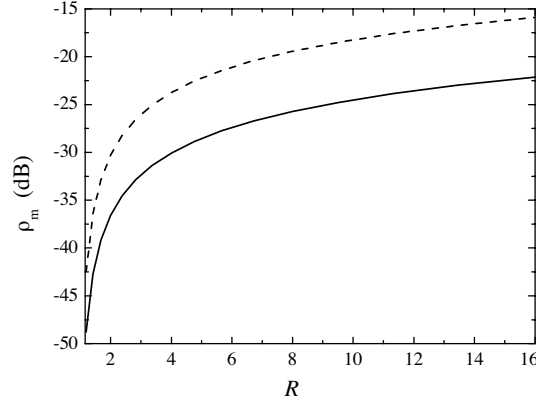


**Figure 2.** Passband tolerance vs.  $R$  for the dual-band transformer (solid line) and the single-band transformer with passband  $[\theta_1 - \Delta\theta, \theta_2 + \Delta\theta]$  (dashed line) for  $N = 4$ ,  $\theta_2/\theta_1 = 2.5$  and  $\Delta\theta/\theta_1 = 0.2$ .

dual-band transformer and the single-band transformer increases, as illustrated in Fig. 3, for  $R = 4$ ,  $\theta_2/\theta_1 = 2.5$  and  $\Delta\theta/\theta_1 = 0.2$ . At  $N = 8$  the dual-band transformer outperforms the single-band transformer by about 13 dB.

The higher the ratio  $\theta_2/\theta_1$  of the two center band frequencies, the larger the difference between the two transformers performance in terms of  $\rho_m$ . This is illustrated in Fig. 4 where the  $\rho_m$  of the dual-

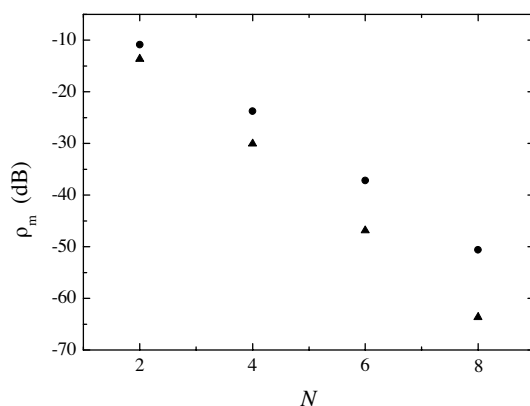


**Figure 3.** Passband tolerance vs.  $N$  for the dual-band transformer (triangles) and the single-band transformer with passband  $[\theta_1 - \Delta\theta, \theta_2 + \Delta\theta]$  (circles) for  $R = 4$ ,  $\theta_2/\theta_1 = 2.5$  and  $\Delta\theta/\theta_1 = 0.2$ .

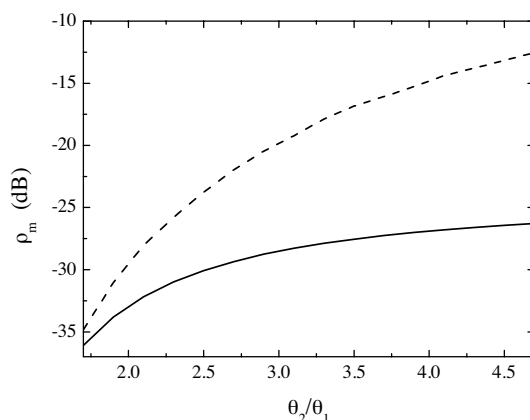


**Figure 4.** Passband tolerance vs.  $\theta_2/\theta_1$  for the dual-band transformer (solid line) and the single-band transformer with passband  $[\theta_1 - \Delta\theta, \theta_2 + \Delta\theta]$  (dashed line) for  $N = 4$ ,  $R = 4$  and  $\Delta\theta/\theta_1 = 0.2$ .

band transformer and the single-band transformer is displayed as a function of  $\theta_2/\theta_1$  for  $N = 4$ ,  $R = 4$  and  $\Delta\theta/\theta_1 = 0.2$ . The  $\rho_m$  of both transformers increases with  $\theta_2/\theta_1$ , while the difference increases from 1.3 dB to 13.7 dB with  $\theta_2/\theta_1$  ranging from 1.7 to 4.7.

Finally, Fig. 5 shows the passband tolerance  $\rho_m$  of the dual-band transformer and the single-band transformer as a function of  $\Delta\theta/\theta_1$  for  $N = 4$ ,  $R = 4$  and  $\theta_2/\theta_1 = 2.5$ . For low values of  $\Delta\theta/\theta_1$  the dual-band

transformer exhibits very low values of  $\rho_m$  outperforming the single-band transformer by about 38.5 dB. Both the dual-band transformer and the single-band transformer  $\rho_m$  increase with  $\Delta\theta/\theta_1$  while the difference decreases up to zero for  $\Delta\theta/\theta_1 = 0.75$ , corresponding to  $\theta_1 + \Delta\theta = \theta_2 - \Delta\theta$ .

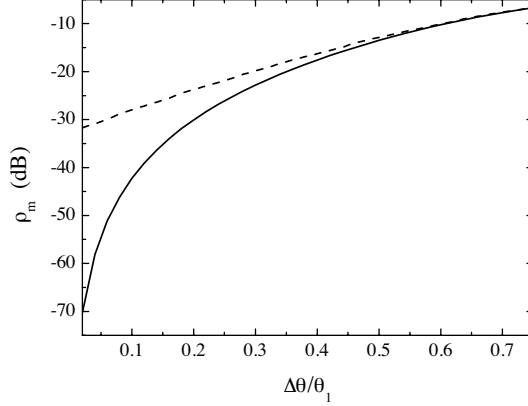


**Figure 5.** Passband tolerance vs.  $\Delta\theta/\theta_1$  for the dual-band transformer (solid line) and the single-band transformer with passband  $[\theta_1 - \Delta\theta, \theta_2 + \Delta\theta]$  (dashed line) for  $N = 4$ ,  $R = 4$  and  $\theta_2/\theta_1 = 2.5$ .

We also compared the dual-band transformer to the single-band transformer with center frequency  $f_0$  and the same tolerance  $\rho_m$  in terms of their passbands. Dual-band transformer and single-band transformer input reflection coefficient absolute values are shown in Fig. 6 for  $R = 4$ ,  $N = 4$ ,  $\theta_2/\theta_1 = 2.5$  and  $\Delta\theta/\theta_1 = 0.2$ . The single-band transformer is forced to have the same passband tolerance of the dual-band transformer, namely  $\rho_m = -30.06$  dB. It is seen in Fig. 6 that the single-band transformer does not cover both passbands of the dual-band transformer. The same behavior has been observed also varying the parameters  $R$ ,  $N$ ,  $\theta_2/\theta_1$  and  $\Delta\theta/\theta_1$ . Figs. 7 and 8 show the ratio of the single-band transformer passband  $\Delta\bar{\theta}$  to  $\Delta\Theta = (\theta_2 + \Delta\theta) - (\theta_1 - \Delta\theta)$  as a function of  $\theta_2/\theta_1$  and  $\Delta\theta/\theta_1$ , respectively. As expected,  $\Delta\bar{\theta}/\Delta\Theta$  decreases with  $\theta_2/\theta_1$  and increases with  $\Delta\theta/\theta_1$ . In all simulations performed varying  $R$  from 1.1 to 16 and  $N$  from 2 to 8,  $\Delta\bar{\theta}/\Delta\Theta$  keeps around 0.85 for  $\theta_2/\theta_1 = 2.5$  and  $\Delta\theta/\theta_1 = 0.2$ .

Moreover, it is worth to analyze the characteristic impedance values of the transformer sections obtained using our method. In Table 1(a) the impedance values are reported for the case  $N = 4$ ,  $R = 4$ ,  $\theta_2/\theta_1 = 2.5$  and  $\Delta\theta/\theta_1 = 0.2$ . Table 1(b) shows the impedance values for the same parameter values but for  $\theta_2/\theta_1 = 3.5$ . In the case of



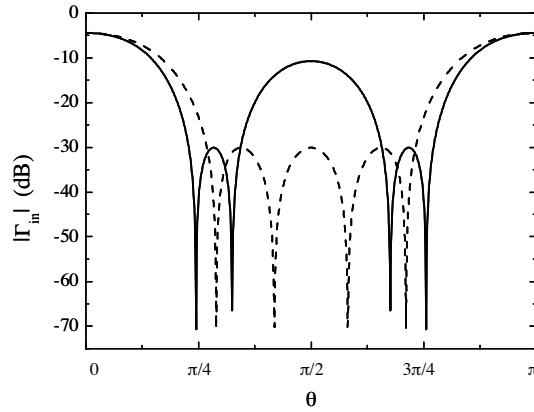


**Figure 6.** Reflection coefficient absolute value vs.  $\theta$  for the dual-band transformer (solid line) and the single-band transformer with the same passband tolerance (dashed line) for  $R = 4$ ,  $N = 4$ ,  $\theta_2/\theta_1 = 2.5$  and  $\Delta\theta/\theta_1 = 0.2$ .

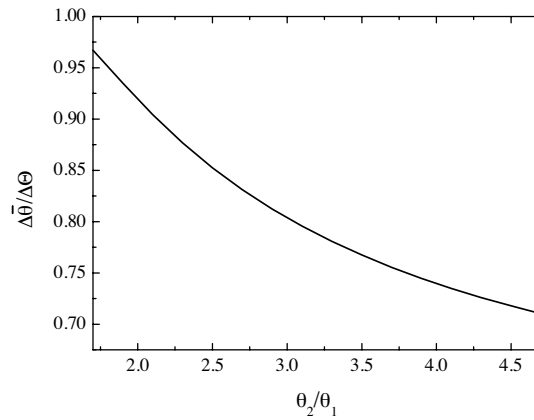


**Figure 7.** Ratio  $\Delta\bar{\theta}/\Delta\theta$  vs.  $\theta_2/\theta_1$  for  $N = 4$ ,  $R = 4$  and  $\Delta\theta/\theta_1 = 0.2$ .

Table 1(a), our method gives a transformer with a monotonous step to step impedance variation. On the contrary, in the case of Table 1(b), a transformer with a non-monotonous step to step impedance variation is obtained using our procedure. All the simulations we performed showed that the monotonous/non-monotonous variation depends only on the parameter  $\theta_2/\theta_1$ . In particular, for  $\theta_2/\theta_1 \leq 3$  our method gives a transformer with a monotonous step to step variation, for  $\theta_2/\theta_1 > 3$  a

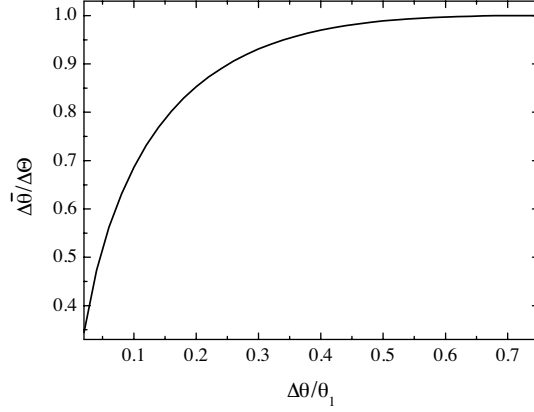


**Figure 8.** Ratio  $\Delta\bar{\theta}/\Delta\theta$  vs.  $\Delta\theta/\theta_1$  for  $N = 4$ ,  $R = 4$  and  $\theta_2/\theta_1 = 2.5$ .

**Table 1.** Characteristic impedance values of the transformer sections for  $N = 4$ ,  $R = 4$ ,  $\Delta\theta/\theta_1 = 0.2$ , (a)  $\theta_2/\theta_1 = 2.5$ , (b)  $\theta_2/\theta_1 = 3.5$ .

	(a)	(b)
	$Z$ [ $\Omega$ ]	$Z$ [ $\Omega$ ]
1st section	64.50	81.41
2nd section	78.53	63.14
3rd section	127.33	158.38
4th section	155.03	122.84

transformer with a non-monotonous step to step variation is obtained. Of course, in both cases the Collin-Riblet condition  $Z_i Z_{N+1-i} = Z_L Z_0$  is always fulfilled [16].

Finally, we conclude the analysis of the performance of our synthesis method analyzing its robustness with respect to the absorption in real materials. For a transmission line consisting of a lossy dielectric material surrounding perfect conductors, assuming a time dependence  $e^{j2\pi ft}$ , the characteristic impedance  $Z'$  and the propagation constant  $k$  are given by [1]

$$Z' = \frac{Z}{(1 - j \tan \delta)^{1/2}} \quad (9)$$

$$k = \beta(1 - j \tan \delta)^{1/2} \quad (10)$$

where  $Z$  and  $\beta$  are the lossless characteristic impedance and propagation constant, respectively, and  $\tan \delta = \epsilon''/\epsilon'$ ,  $\epsilon = \epsilon' - j\epsilon''$  being the relative dielectric constant.

As an example, we analyze the case  $N = 4$ ,  $R = 4$ ,  $\Delta\theta/\theta_1 = 0.2$  and  $\theta_2/\theta_1 = 3.5$ . At first, we apply our method and obtain the characteristic impedance values reported in Table 1(b). Then, we perturb these impedance values following equation (9), and compute the power  $P_L$  delivered to the load considering the corresponding propagation constants given by equation (10).

In Fig. 9,  $P_L$  normalized to the power  $P_G$  available from the generator is displayed as a function of  $\theta$  for four different values of  $\tan \delta = 0, 10^{-3}, 5 \cdot 10^{-3}, 10^{-2}$ . It can be noted that moderate dielectric losses in the transmission line sections do not significantly affect the transformer performance. Obviously, the losses effects are more evident in the higher frequency passband  $\Theta_2$  where, for  $\tan \delta = 10^{-2}$ ,  $P_L$  decreases of about 10%.

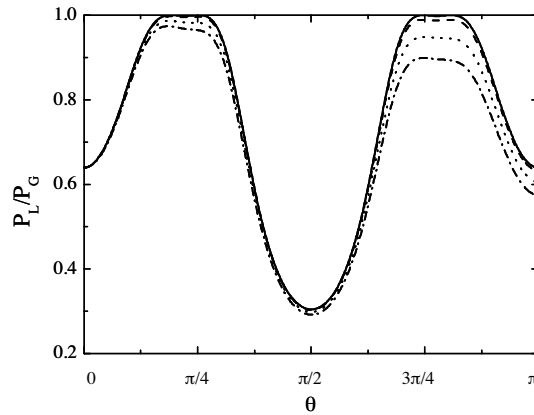


**Figure 9.** Power delivered to the load normalized to the power available from the generator vs  $\theta$ :  $\tan \delta = 0$  (solid line),  $\tan \delta = 10^{-3}$  (dashed line),  $\tan \delta = 5 \cdot 10^{-3}$  (dotted line) and  $\tan \delta = 10^{-2}$  (dash-dotted line) for  $N = 4$ ,  $R = 4$ ,  $\Delta\theta/\theta_1 = 0.2$  and  $\theta_2/\theta_1 = 3.5$ .

#### 4. MICROSTRIP TRANSFORMERS

The method presented and discussed in the previous sections works in the case of TEM propagation in transmission lines. On the other hand, wave-guiding structures supporting not-TEM propagation are being used more and more in current microwave applications. For example, planar microwave circuits based on microstrip lines have

received intensive development in the last few decades [17–19]. A microstrip line supports quasi-TEM mode propagation which can be approximated by TEM propagation in a transmission line with effective dielectric constant and characteristic impedance evaluated via a quasi-static approximation [2]. In this section we demonstrate that our method can also be used in the design of a microstrip transformer, showing that quasi-TEM to TEM approximation has negligible effects on the transformer performance.

Let us consider the problem of synthesizing a microstrip transformer matching, in two separate bands, a given microstrip line to a known planar load  $Z_L$ . Given the height and the dielectric constant of the substrate, the design procedure consists in finding out the widths of the microstrip sections. At first, we compute the characteristic impedance of the transmission line equivalent to the input microstrip line using the quasi-static approximation formulas reported in [2]. Then, using our method, we perform the synthesis of the transformer matching the equivalent transmission line to a load of impedance  $Z_L$  in the two desired bands, obtaining the characteristic impedances  $Z_i$  ( $i = 1, \dots, N$ ) of the transformer sections. Finally, using again the quasi-static approximation formulas, we compute the widths of the  $N$  sections of the microstrip transformer corresponding to the  $Z_i$  ( $i = 1, \dots, N$ ). The performance of the microstrip transformer is then analyzed via a full-wave commercial software package [20].

As a first example, we consider a microstrip line with a substrate consisting of 0.20 mm height RT/duroid 5880 having relative dielectric constant equal to 2.2. The width of the microstrip line is  $w = 0.62$  mm, corresponding to a characteristic impedance  $Z_0 = 50 \Omega$ , the load impedance is  $Z_L = 200 \Omega$ . At first, we consider the problem faced in the first case of Section 3, for which  $R = 4$ ,  $N = 4$ ,  $\theta_2/\theta_1 = 2.5$  and  $\Delta\theta/\theta_1 = 0.2$ , giving a transformer with monotonous step to step impedance variation. The input reflection coefficient absolute value  $|\Gamma_{in}|$  of the microstrip transformer, computed via the full-wave analysis, is compared with the  $|\Gamma|$  given by Equation (8) in Fig. 10, where  $|\Gamma|$  and  $|\Gamma_{in}|$  are displayed as functions of  $\theta$ . As it can be seen, the  $|\Gamma_{in}|$  profile well agrees with the  $|\Gamma|$  one. As a further example, we consider the matching problem with parameter values as above but for  $\theta_2/\theta_1 = 3.5$ , giving a transformer with a non-monotonous step to step impedance variation as shown in Section 3.  $|\Gamma|$  and  $|\Gamma_{in}|$  are displayed in Fig. 11, showing a very good agreement between the two profiles also in this case.

All simulations performed using different parameter values confirmed these results.

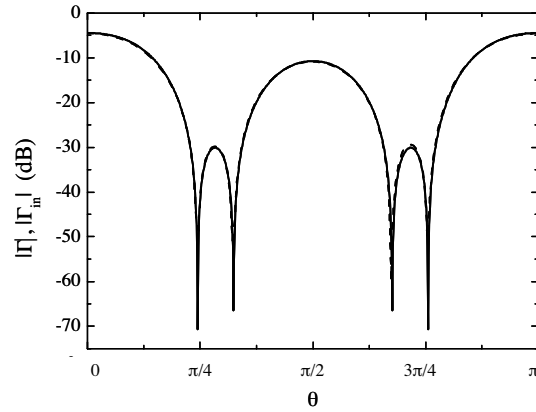


**Figure 10.** Reflection coefficient absolute value vs.  $\theta$ : theoretical values  $|\Gamma|$  (solid line) and full-wave analysis values  $|\Gamma_{in}|$  (dashed line) for  $R = 4$ ,  $N = 4$ ,  $\theta_2/\theta_1 = 2.5$  and  $\Delta\theta/\theta_1 = 0.2$ .

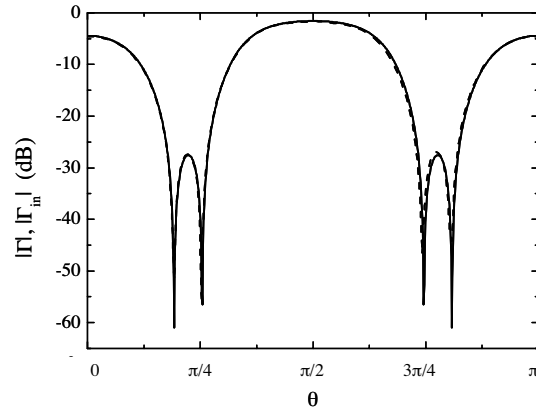


**Figure 11.** Reflection coefficient absolute value vs.  $\theta$ : theoretical values  $|\Gamma|$  (solid line) and full-wave analysis values  $|\Gamma_{in}|$  (dashed line) for  $R = 4$ ,  $N = 4$ ,  $\theta_2/\theta_1 = 3.5$  and  $\Delta\theta/\theta_1 = 0.2$ .

## 5. CONCLUSIONS

We have introduced a new exact synthesis method of multisection impedance transformers for transmission line circuits supporting TEM propagation. Our method allows the design of dual-band transformers with  $N = 2M$  sections working in two bands  $\Omega_1$  and  $\Omega_2$  centered at two arbitrary frequencies  $f_1$  and  $f_2$ , respectively, without any

restriction on  $M$  and on the values of the impedances to be matched. In terms of passband tolerance in the two required bands  $\Omega_1$  and  $\Omega_2$ , our transformer, which consists of a cascade of uniform transmission line sections which are a quarter wave long at the frequency  $f_0 = (f_1 + f_2)/2$ , outperforms the exact single-band Chebyshev transformer whose passband encompasses both  $\Omega_1$  and  $\Omega_2$ , which is perhaps the most obvious alternative design. We have also explored the possibility of using our synthesis in the case of waveguiding structures supporting quasi-TEM propagation, showing that our method gives very good results in designing impedance transformers for microstrip circuits.

## REFERENCES

1. Collin, R. E., *Foundations for Microwave Engineering*, 2nd edition, McGraw-Hill, New York, 1992.
2. Pozar, D. M., *Microwave Engineering*, 2nd ed., John Wiley & Sons Inc., New York, 1998.
3. Bandler, J. W. and P. A. Macdonald, "Optimization of microwave networks by razor search," *IEEE Trans. Microwave Theory Tech.*, Vol. 17, No. 8, 552–562, 1969.
4. De Coster, I., E. Van Lil, and A. Van de Capelle, "Comparison of design methods for binomial matching transformers," *Journal of Electromagnetic Waves and Applications*, Vol. 14, No. 9, 1229–1239, 2000.
5. Meschanov, M. P., I. A. Rasukova, and V. D. Tupikin, "Stepped transformers on TEM-transmission lines," *IEEE Trans. Microwave Theory Tech.*, Vol. 44, No. 6, 793–798, 1996.
6. Wu, G.-L., W. Mu, X.-W. Dai, and Y.-C. Jiao, "Design of novel dual-band bandpass filter with microstrip meander-loop resonator and CSRR DGS," *Progress In Electromagnetics Research*, PIER 78, 17–24, 2008.
7. Ren, W., "Compact dual-band slot antenna for 2.4/5 GHz WLAN applications," *Progress In Electromagnetics Research B*, Vol. 8, 319–327, 2008.
8. Fan, J.-W., C.-H. Liang, and X.-W. Dai, "Design of cross-coupled dual-band filter with equal-length split-ring resonators," *Progress In Electromagnetics Research*, PIER 75, 285–293, 2007.
9. Zhao, G., F.-S. Zhang, Y. Song, Z.-B. Weng, and Y.-C. Jiao, "Compact ring monopole antenna with double mender lines for 2.45/5 GHz dual-band operation," *Progress In Electromagnetics Research*, PIER 72, 187–194, 2007.
10. Chow, Y. L. and K. L. Wan, "A transformer of one-third

- wavelength in two sections — for a frequency and its first harmonic,” *IEEE Microwave Wireless Comp. Lett.*, Vol. 12, No. 1, 22–23, 2002.
11. Monzon, C., “Analytical derivation of a two-section impedance transformer for a frequency and its first harmonic,” *IEEE Microwave Wireless Comp. Lett.*, Vol. 12, No. 10, 381–382, 2002.
  12. Monzon, C., “A small dual-frequency transformer in two sections,” *IEEE Trans. Microwave Theory Tech.*, Vol. 51, No. 4, 1157–1161, 2003.
  13. Orfanidis, S. J., “A two-section dual-band Chebyshev impedance transformer,” *IEEE Microw. Wireless Comp. Lett.*, Vol. 13, No. 9, 382–384, 2003.
  14. Castaldi, G., V. Fiumara, and I. M. Pinto, “A dual-band Chebyshev impedance transformer,” *Microwave and Optical Technol. Lett.*, Vol. 39, No. 2, 141–145, 2003.
  15. Collin, R. E., “Theory and design of wide-band multisection quarter-wave transformers,” *Proc. IRE*, Vol. 43, No. 2, 179–185, 1955.
  16. Riblet, H. J., “General synthesis of quarter-wave impedance transformers,” *IRE Trans. Microwave Theory Tech.*, Vol. 5, No. 1, 36–43, 1957.
  17. Khalaj-Amirhosseini, M., “Wideband or multiband complex impedance matching using microstrip nonuniform transmission lines,” *Progress In Electromagnetics Research*, PIER 66, 15–25, 2006.
  18. Kiang, J. F., S. M. Ali, and J. A. Kong, “Modelling of lossy microstrip lines with finite thickness,” *Progress In Electromagnetics Research*, PIER 4, 85–117, 1991.
  19. Matsunaga, M., “A coupled-mode theory-based analysis of coupled microstrip lines on a ferrite substrate,” *Progress In Electromagnetics Research*, PIER 42, 219–232, 2003.
  20. CST Microwave Studio Suite, Getting started version 4, 2002.